# scientific reports

OPEN

# Network pharmacology combined with GEO database identifying the mechanisms and molecular targets of Polygoni Cuspidati Rhizoma on Peri-implants

Chao Shan[1,2], Xiaowei Ji[1,2], Zeyu Wu[1,2] & Jin Zhao[1,2,3]✉

Peri-implants is a chronic disease leads to the bone resorption and loss of implants. Polygoni Cuspidati Rhizoma (PCRER), a traditional Chinese herbal has been used to treat diseases of bone metabolism. However, its mechanism of anti-bone absorption still remains unknown. We aimed to identify its molecular target and the mechanism involved in PCRER potential treatment theory to Peri-implants by network pharmacology. The active ingredients of PCRER and potential disease-related targets were retrieved from TCMSP, Swiss Target Prediction, SEA databases and then combined with the Peri-implants disease differential genes obtained in the GEO microarray database. The crossed genes were used to protein–protein interaction (PPI) construction and Gene Ontology (GO) and KEGG enrichment analysis. Using STRING database and Cytoscape plug-in to build protein interaction network and screen the hub genes and verified through molecular docking by AutoDock vina software. A total of 13 active compounds and 90 cross targets of PCRER were selected for analysis. The GO and KEGG enrichment analysis indicated that the anti-Peri-implants targets of PCRER mainly play a role in the response in IL-17 signaling, Calcium signaling pathway, Toll-like receptor signaling pathway, TNF signaling pathway among others. And CytoHubba screened ten hub genes (MMP9, IL6, MPO, IL1B, SELL, IFNG, CXCL8, CXCL2, PTPRC, PECAM1). Finally, the molecular docking results indicated the good binding ability with active compounds and hub genes. PCRER's core components are expected to be effective drugs to treat Peri-implants by anti-inflammation, promotes bone metabolism. Our study provides new thoughts into the development of natural medicine for the prevention and treatment of Peri-implants.

Peri-implant, which refers to inflammatory damage to the hard and soft tissues around implants, including peri-implant mucositis and peri-implants inflammation. Peri-implant mucositis is limited to the surrounding soft tissue, rather Peri-implants could penetrate into the implants and cause severe bone resorption, if left untreated, can cause the loss of the implant[1]. Recent studies have shown that up to 56% of implant patients and even 43% of implant sites are affected by Peri-implants[2].

Peri-implants is mainly manifested as soft tissue inflammation, abscess and fistula formation[3]. Subgingival plaque is the main pathogenic cause of this disease, and the pathogenic bacteria are mainly anaerobic bacteria such as Fusobacterium nucleatum, Porphyromonas gingivalis, Actinobacillus actinomycetemcomitan, etc. Huge of systemic and local factors, including pathogenic bacteria, poor oral hygiene, smoking and alcohol consumption are associated with the development of Peri-implants[4]. There are similarities and differences in understanding and treatment of implants in traditional Chinese and Western medicine. In western medicine, both Peri-implants and periodontitis are infectious diseases caused by plaque microorganisms. Therefore, the treatment of Peri-implants mainly involves long-term application of a large number of antibacterial drugs to combat bacterial inflammatory destruction, degradation of collagen fibers and matrix, so as to eliminate periodontal pocket and restore the bone loss[5]. Minocycline hydrochloride, could inhibit collagen enzyme activity, has the excellent affinity with

[1]Department of Dentistry, Xinjiang Medical University, Ürümqi, China. [2]The First Affiliated Hospital of Xinjiang Medical University (Affiliated Stomatology Hospital), Ürümqi, China. [3]Xinjiang Uygur Autonomous Region Institute of Stomatology, Ürümqi, China. ✉email: zhaojin@xjmu.edu.cn

osseous tissue and has a wide antimicrobial spectrum strong sterilization activity, it also prompts the implant surrounding soft tissue regeneration because of its ideal permeability[6,7]. But the use of antibiotics often brings many adverse reactions, such as allergic reactions, gastrointestinal reactions and so on[8].

Traditional Chinese Medicine (TCM) has been used in China for thousand years, which has a multi-target therapeutic effect on a variety of diseases, including complex bone metabolic diseases, such as osteoporosis and periodontitis[9,10]. For a long time, Polygoni Cuspidati Rhizoma Et Radix(PCRER) was considered as an invasive plant in Europe and North America, but its recent inclusion in the European Pharmacopoeia makes it possible to use it as a traditional plant medicine[11]. PCRER mainly contains anthraquinones, stilbenes and some fatty acid compounds, which has a variety of pharmacological effects, including anti-inflammatory, antiviral, anti-apoptotic, regulating blood lipids, anti-thrombosis, myocardial protection, anti-oxidation, anti-tumor and other pharmacological effects. As a traditional Chinese medicine, PCRER was often used in combination with different TCMs to treat liver injury, chronic pelvic inflammatory disease, acne, menstrual irregularities, burns, and arthritis etc.[12–14]. Some studies have reported that extracts of PCRER or its main compounds have antioxidant and antibacterial effects and it was used in Korea, China and Japan to treat osteomyelitis[15,16]. It has also been proved having antibacterial activity against Streptococcus mutans and was used by civilian medical organizations to maintain oral hygiene in South Korea[17,18]. Hadzik et al. obtained extracts of PCRER with the highest bacteriostatic and bactericidal activities against the caries-pathogens, especially to streptococcus. In addition, the cytotoxicity of PCRER's extracts to S. mutans was low at antibacterial concentration, and appears to have stimulating effect on normal human fibroblasts, which may accelerate the healing of gingival wounds[19]. At present, there are amount of experiments on treating peri-implants with Traditional Chinese medicine or PCRER's compounds such as Mangiferin[20], Cranberry[21], Quercetin[22], Resveratrol[23]. However, the specific mechanism of treatment of peri-implants with PCRER is still unclear.

Before the term "network pharmacology" was proposed, the study of TCM and biological network appeared for the first time in 2007 proposed by Shao Li who who laid a foundation for the establishment of new research strategies of biological network and TCM[24]. The mode of "network target, multi-component" was taken as the core concept of network pharmacology of TCM[25].Bio-information network construction and network topology analysis strategies based on high-throughput data analysis, virtual computing and network database retrieval can systematically clarify the molecular mechanism of TCM treatment of various diseases, and a huge of studies have been published[26,27]. Network pharmacology uses artificial intelligence to predict drug targets and binding patterns, identify biomarkers for diseases and syndromes, retarget drugs, and use algorithms and big data at its core to understand the occurrence and progression of disease and syndrome[28]. Therefore, in this study, we combined the web-based pharmacology approach with the Gene Expression Omnibus Database (GEO), the potential mechanism was explored through GO&KEGG pathway analysis, and the "hub genes" of PCRER treatment of Peri-implants were screened, to clarify the comprehensive mechanism of PCRER against peri-implants.

## Materials and methods

**Establishment of the component database of PCRER.** The ingredients of PCRER were obtained from TCMSP (http://lsp.nwu.edu.cn/tcmsp.php) database. The TCMSP database provides information on Chinese herbal medicines from the Chinese Pharmacopoeia, as well as drug chemistry, drug similarity, drug target, disease targeted by each active compound, and other relevant information[29]. OB stands for the efficiency with which bioactive ingredients enter the systemic circulation, while DL represents the qualitative indicator that is applied to drug design to estimate similarities between ingredients and certified drug structures. We selected drug similarity characteristics and oral bioavailability as conditions, where (DL) ≥ 0:18, (OB) ≥ 30%[30], and the active components of PCRER reported in literature were also included in the database.

**Component of PCRER target fishing.** Targets for major compounds in PCRER were identified and implemented by the following database TCMSP, Swiss Target Prediction (http://www.Swisstargetprediction.ch/)[31], SEA (https://sea.bkslab.org/[32]. Meanwhile, UniProt database (https://www.uniprot.org/) was used for target information comparison and gene name standardization. After the targets in the above three databases were combined and deleted the duplicate values, putative targets of PCRER were obtained.

**Establish the targets database of Peri-implants.** Few targets related to Peri-implants can be found in the current epidemic disease database, so we chose the GEO database (http://www.ncbi.nlm.nih.gov/geo) to construct our research database by analyzing differentially expressed microarrays. The search strategy ('Peri-implants' [All Fields]) AND ('Homo sapiens'[Organism] AND 'Expression profiling by array'[Filter]) was adopted. Expression profiling data from GSE178351, GSE57631 and GSE106090 were downloaded from the GEO database based on the microarray platform GPL23159, GPL15034(both from Affymetrix Human Gene Expression Array) and GPL21827(Agilent Human Gene Expression Array). Gene IDs were identified according to the platform annotation probe ID information. DEGs between patients with Peri-implants and healthy individuals were screened using the 'limma' package of R software (version 3.6.3) according to $P < 0.05$, and |$\log_2$ fold change (FC)|> 1. Then, the volcano plot and heatmaps of DEGs from three dataset were plotted by the 'Pheatmap' and 'ggplot' package in the R software. Finally, we combined the differential genes in the three data sets, deleted the duplicate values, and established the gene target database of peri-implantitis after standardization with Uniprot database.

**Construction of "PCRER-component-target" Peri-implants network.** We obtained the target genes of the active components of PCRER and the therapeutic targets of Peri-implants from the above four databases and obtained overlapping genes, integrated network information on ingredients, genes and disease

targets. Finally, we use Cytoscape software (V.3.7.2, https://cytoscape.org/) to conduct network topology analysis on these data and construct P-C-T-P network.

**GO and KEGG enrichment analysis.** 'org.hs.eg. Db', 'stringi', 'ClusterProfiler' and 'ggplot2' of the R package was installed in software R 3.6.3 for enrichment analysis of GO and Kyoto Encyclopedia of Genes and Genomes (KEGG). Go enrichment analysis was carried out with the function of "Enrichment go". KEGG enrichment analysis carried the enrich-KEGG function and the database was KEGG database (https://www.kegg.Jp/[33]. For parameters of both species was HAS and filter values (P and Q values) are set to 0.05. The first 15 enrichment results were output to draw bubble graphs, bar graphs and circos graphs of GO-BP, GO-CC, GO-MF and KEGG regulatory networks. And KEGG pathway enrichment network map with crossover genes was generated by Cytoscape 3.7.2 software.

**Core target screening of PCRER treatment for Peri-implants.** Enter overlapping targets of PCRER/Peri-implants into STRING database (http://www.string-db.org/), the target-target interaction network, target interaction in protein–protein interaction (PPI) network diagram (with an overall score > 0.4 as interception criteria) and. tsv data were obtained[34]. Next, to further identify the core therapeutic targets, Cytoscape plug-in MCODE (Molecular Complex Detection) was used to identify significant modules (MCODE score ≥ 4) and another plug-in Cytohubba was used. MCC algorithm was used to study node degree (score ≥ 10) of key nodes in significant modules[35], the hub genes contained in PPI network was screened.

**Molecular docking verification of PCRER binding to hub protein.** Molecular docking refers to process in which two or more molecules identify each other through geometric matching and energy matching, including electrostatic interaction, hydrogen bonding, van der Waals interaction and hydrophobic interaction. In the field of drug design, the purpose of molecular docking was to find the best binding position and binding conformation between small molecule and target enzyme protein[36]. In order to assess the credibility of the association between the target and the compound and to identify the new ingredient candidates for the treatment of Peri-implants, we performed molecular docking between the core compound and the core target. Crystal structures of core proteins were downloaded from Protein Data Bank (http://www.rcsb.org/pdb) and stored in PDB format. Candidate compounds of two-dimensional (2D) structure was downloaded from the PubChem database (https://pubchem.ncbi.nlm.nih.gov/), save in SDF format. Ligands and receptors were prepared with Chem3D using AutoDock Tools (V. 1.5.6). Among them, the preparation of the receptor includes deleting the original ligand and water molecules from the crystal structure of the receptor, adding non-polar hydrogen, and calculating the partial charge of Gasteiger[37]. The process for handling ligands involves applying energy to minimize and distribute atomic charges and atoms. All prepared receptors and ligands are stored in PDBQT format. Then, Autodock Vina was used for molecular docking, and the docking center was set by the grid box function in the software[38]. The best docking position was the one with the minimum root mean square deviation (RMSD) predicted by X-ray crystal configuration, and the affinity between ligand and target protein was evaluated to indicate the binding strength. Affinity < − 5.00 kcal/mol indicates good binding strength, and affinity < − 7.00 kcal/mol indicates good binding strength. The docking conformation was visualized by Pymol 2.3.

**Ethical declaration.** All data used in this study came from public databases and does not include any studies related to animals or humans.

## Results

**Screening of active compounds and targets.** A total of 87 active ingredients were obtained from TSMSP platform and 13 core active compounds were selected according to the screening criteria of ADME model, including 6,8-Dihydroxy-7-methoxyxanthone, Physovenine, Picralinal, Physcion- diglucoside, rhein, Torachrysone-8-O-beta-D-(6'-oxayl)-glucoside, beta-sitosterol, (+)-catechin, luteolin, quercetin, resveratrol, polydatin, emodin. The molecular ID, ingredients names and ADME-related parameters are listed in Table 1. According to the Canonical SMILES number of core active compounds of PCRER, after removing duplicate genes, 930 PCRER targets were identified by combing the results obtained from TCMSP, SEA and Swiss target prediction databases, Moreover, the UniProt database was used to acquire the Uniprot IDs of potential targets so that they could be used for further network construction (Supplementary Table S1).

**Identification of Peri-implants-Related Targets.** Different genetic analysis between Peri-implants and healthy individuals was performed with $|\log_2 FC| > 1$ and $P < 0.05$. Joint analysis of gene chips in the GEO database (GSE178351, GSE57631, GSE106090) contained 11 samples from healthy individuals and 16 Peri-implants patients which identified 1398 differentially expressed genes related to Peri-implants (Supplementary Table S2), volcano plot of the distribution of three dataset's DEGs are shown in Fig. 1, the heatmap of the three data sets are shown in Fig. 2, the quality assessment results of the three data sets are shown in Figure S1.

**Construction of the compound-target regulatory network.** The core active component targets of PCRER were matched with the disease targets of Peri-implants, resulting in the selection of 90 core targets of PCRER and Peri-implants (Fig. 3a) (Table 2). Cytoscape 3.7.2 showed that the targeting relationship between PCRER's active ingredients and intersection genes that presented by the PCRER compound-target regulatory network. (Fig. 3b) including 71 nodes and 286 edges. Active ingredients of quercetin and resveratrol have the most amount of and related target genes, indicating that quercetin and resveratrol in PCRER are the most effica-

| ID | Compound | OB (%) | DL |
|---|---|---|---|
| MOL013281 | 6,8-Dihydroxy-7-methoxyxanthone | 35.82614 | 0.21218 |
| MOL013287 | Physovenine | 106.2136 | 0.18963 |
| MOL013288 | Picralinal | 58.00695 | 0.7541 |
| MOL002259 | Physciondiglucoside | 41.64856 | 0.63145 |
| MOL002268 | Rhein | 47.06521 | 0.27678 |
| MOL002280 | Torachrysone-8-O-beta-D-(6'-oxayl)-glucoside | 43.01996 | 0.73687 |
| MOL000358 | Beta-sitosterol | 36.91391 | 0.75123 |
| MOL000492 | (+)-catechin | 54.82643 | 0.24164 |
| MOL000006 | Luteolin | 36.16263 | 0.24552 |
| MOL000098 | Quercetin | 46.43335 | 0.27525 |
| MOL012744 | Resveratrol | 19.07304 | 0.1093 |
| MOL013289 | Polydatin | 21.44273 | 0.49765 |
| MOL000472 | Emodin | 24.39832 | 0.23916 |

**Table 1.** The total available compounds of Polygoni Cuspidati.



GSE178351          GSE57631          GSE106090
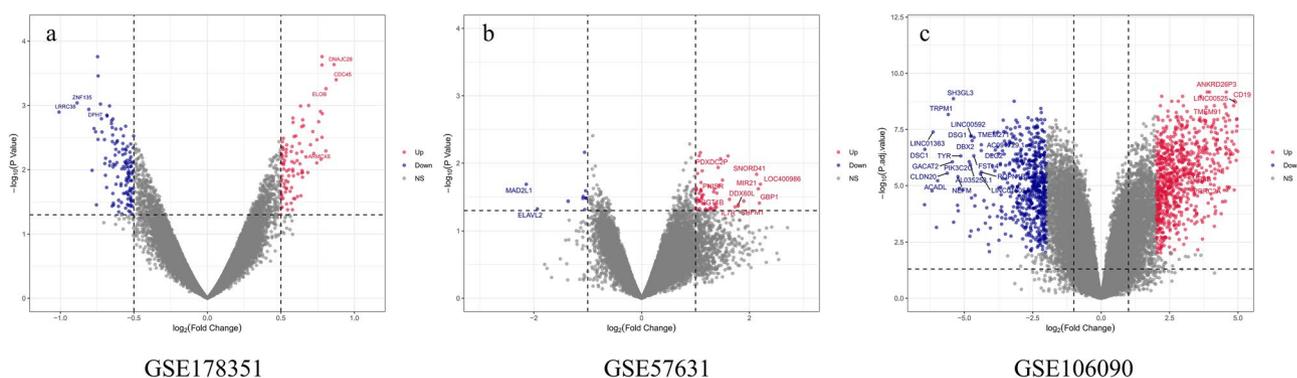
**Figure 1.** Volcano plot of the distribution of low expression of genes in patients with CP. DEGs (**a** GSE178351, **b** GSE57631, **c** GSE106090), Red represents high expression of genes in patients with Peri-implants, while blue represents lower expression of genes (R 3.6.3 https://cran.r-project.org/bin/windows/base/old/3.6.3/).



GSE178351          GSE57631          GSE106090
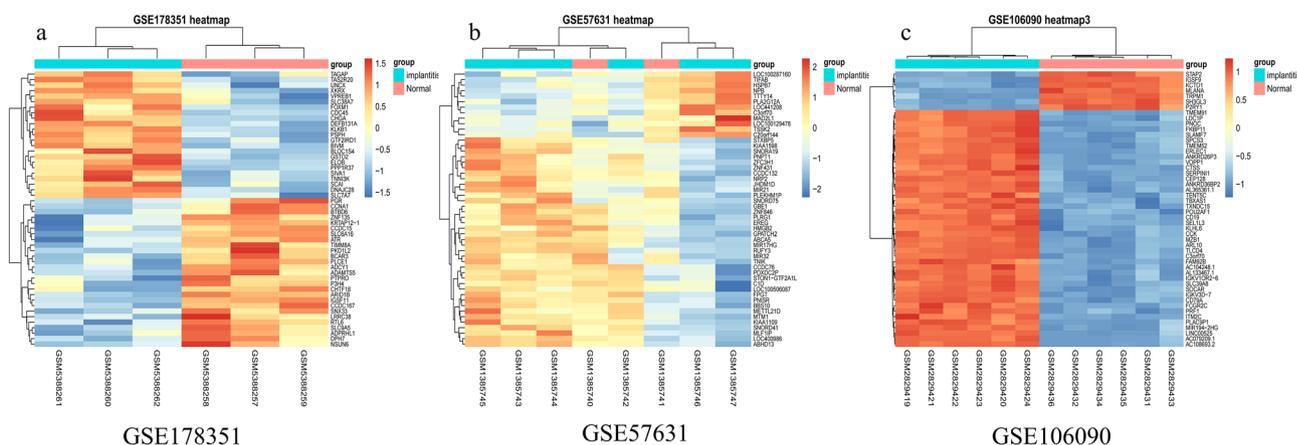
**Figure 2.** Heatmap of the top 50 up- and down-regulated genes (**a** GSE178351, **b** GSE57631, **c** GSE106090). Legend on the top right indicates the log fold change of the genes.

cious components. The target MMP9, IL6, which has the most ligands with the active components, followed by IL1B and MPO.

**Enrichment analysis of the core network.** To further evaluate the 90 candidate targets and related pathways, enrichment analysis was performed using the package 'clusterProfiler' in R. GO enrichment analysis showed that 90 genes were significantly enriched in 394 GO items in the core network, including 13 in BP, 51

**Figure 3.** (**a**) 90 crossed targets common between the predicted PCRER targets and the Peri-implants-associated targets. (**b**) Network of targets predicted using the PCRER-derived compounds. Green nodes represent the active compounds, whereas the Lake blue nodes represent the predicted targets. These edges represent the interaction between the compounds and the targets, and the node size is proportional to the degree of interaction (Cytoscape 3.7.2 https://cytoscape.org/).

in CC, and 328 in MF. Detailed information on GO analysis is presented in Table S3. Moreover, the top 15 most enriched GO terms are presented in Fig. 4. In terms of molecular function, PCRER treatment of Peri-implants mainly involves cell metabolism, proliferation which needs the further experiments to verify, such as regulation of cell growth (GO: 0001558), cell growth (GO: 0016049), cellular divalent inorganic cation homeostasis (GO: 0072503), regulation of inflammatory response (GO: 0050727); In terms of biological processes, the core targets are enriched in membrane function: membrane raft (GO:0045121), membrane microdomain (GO:0098857), membrane region (GO:0098589), apical plasma membrane (GO:0016324). As for cellular components, the genes are mainly clustered in kinase activity such as protein tyrosine kinase activity (GO:0004713), endopeptidase activity (GO:0004175), transmembrane receptor protein kinase activity (GO:0019199). In addition, based on the analysis of KEGG, a gene-pathway network was established and the corresponding target genes and screened the first 20 pathways related to Peri-implants with significantly enriched $P$ value which are displayed in Fig. 5. including IL-17 signaling pathway (hsa04657), Transcriptional misregulation in cancer (hsa05202), Rheumatoid arthritis (hsa05323), Bladder cancer (hsa05219), Lipid and atherosclerosis (hsa05417), Calcium signaling pathway (hsa04020), TNF signaling pathway (hsa04668), Toll-like receptor signaling pathway (hsa04620) among others. The core network diagram of "Core targets with KEGG_ pathways" was shown in Fig. 6[39].

**PPI network analysis and hub gene verification.** The PCRER-Peri-implants cross targets identified were input into STRING, to remove the unconnected target, and the preliminary PPI network was obtained (interaction score ≥ 0.4). (Supplementary Fig. S2). The origin PPI network of the anti-Peri-implants targets of PCRER) obtained from the STRING database was complex. Therefore, a second network was constructed using the .tsv file and input in Cytoscape (version 3.7.2) to obtain a better visualization. The plug-in MCODE was applied to identify the most enriched module (K score ≥ 4) (Fig. 7a). The top ten hub genes selected by the MCC method (score ≥ 10,000, one of the algorithms in the plug-in Cytohubba)[40] and node degree (score ≥ 10) was screened including IL1B, IL6, CXCL8, IFNG, MMP9, PTPRC, PECAM1, CXCL2, SELL, MPO (Fig. 7b).

**Molecular docking verification.** Molecular docking is a bioinformatic tool that refers to the use of computer technology simulation ligand (protein, DNA/RNA, small molecule) and the receptor protein biological macromolecules in combination with each other, and calculated its mode and affinity according to the physical and chemical parameters through geometric matching and energy between molecules, looking for the best combination of small molecules (the ligand) and biological macromolecules (receptors) of process.

Through PPI network analysis and target screening we screened ten Hub genes were used as docking ligands. Then we screened out components that might be combined with Hub gene from the target database of compounds for one-to-one docking. The free binding energy of target proteins with their corresponding active compounds were displayed in Table 3. The binding energy of the ligand was less than − 5 kcal/mol, indicating that the binding activity between the receptor and ligand was good[40]. According to the results of molecular docking, the binding energy of most receptor-ligand is less than or equal to − 5 kal/mol. At the same time, through conformational analysis of molecular docking structure, all receptors can form good docking pockets, all ligand

| Symbol | Uniprot | Protein name |
|---|---|---|
| CLK4 | Q9HAZ1 | Dual specificity protein kinase CLK4 |
| SENP7 | Q9BQF6 | Sentrin-specific protease 7 |
| HDAC2 | Q92769 | Histone deacetylase 2 |
| PGGT1B | P53609 | Geranylgeranyl transferase type-1 subunit beta |
| ELANE | P08246 | Neutrophil elastase |
| NAALAD2 | Q9Y3Q0 | N-acetylated-alpha-linked acidic dipeptidase 2 |
| ADAMTS5 | Q9UNA0 | A disintegrin and metalloproteinase with thrombospondin motifs 5 |
| CA9 | Q16790 | Carbonic anhydrase 9 |
| TNNC1 | P63316 | Troponin C, slow skeletal and cardiac muscles |
| OPRD1 | P41143 | Delta-type opioid receptor |
| BRCA1 | P38398 | Breast cancer type 1 susceptibility protein |
| PPARG | P37231 | Peroxisome proliferator-activated receptor gamma |
| NOS2 | P35228 | Nitric oxide synthase, inducible |
| CD80 | P33681 | T-lymphocyte activation antigen CD80 |
| IGFBP6 | P24592 | Insulin-like growth factor-binding protein 6 |
| PGR | P06401 | Progesterone receptor |
| ESR1 | P03372 | Estrogen receptor |
| IFNG | P01579 | Interferon gamma |
| CDC45 | O75419 | Cell division control protein 45 homolog |
| PDE10A | Q9Y233 | cAMP and cAMP-inhibited cGMP 3',5'-cyclic phosphodiesterase 10A |
| CA14 | Q9ULX7 | Carbonic anhydrase 14 |
| PIM2 | Q9P1W9 | Serine/threonine-protein kinase pim-2 |
| SLC28A3 | Q9HAS3 | Solute carrier family 28 member 3 |
| SLC22A12 | Q96S37 | Solute carrier family 22 member 12 |
| ESR2 | Q92731 | Estrogen receptor beta |
| NEU4 | Q8WWR8 | Sialidase-4 |
| ST3GAL2 | Q16842 | CMP-N-acetylneuraminate-beta-galactosamide-alpha-2,3-sialyltransferase 2 |
| EPHA7 | Q15375 | Ephrin type-A receptor 7 |
| ELAVL3 | Q14576 | ELAV-like protein 3 |
| PTGDR | Q13258 | Prostaglandin D2 receptor |
| PLA2G7 | Q13093 | Platelet-activating factor acetylhydrolase |
| PDE4B | Q07343 | cAMP-specific 3',5'-cyclic phosphodiesterase 4B |
| BTK | Q06187 | Tyrosine-protein kinase BTK |
| AKR1C1 | Q04828 | Aldo–keto reductase family 1 member C1 |
| CACNA1B | Q00975 | Voltage-dependent N-type calcium channel subunit alpha-1B |
| EPHB3 | P54753 | Ephrin type-B receptor 3 |
| PIK3CG | P48736 | Phosphatidylinositol 4,5-bisphosphate 3-kinase catalytic subunit gamma isoform |
| LGALS7 | P47929 | Galectin-7 |
| MMP13 | P45452 | Collagenase 3 |
| PTGIR | P43119 | Prostacyclin receptor |
| PIGA | P37287 | Phosphatidylinositol N-acetylglucosaminyltransferase subunit A |
| FLT3 | P36888 | Receptor-type tyrosine-protein kinase FLT3 |
| RORA | P35398 | Nuclear receptor ROR-alpha |
| EPHX2 | P34913 | Bifunctional epoxide hydrolase 2 |
| GABRA3 | P34903 | Gamma-aminobutyric acid receptor subunit alpha-3 |
| CCR1 | P32246 | C–C chemokine receptor type 1 |
| SLC6A4 | P31645 | Sodium-dependent serotonin transporter |
| WEE1 | P30291 | Wee1-like protein kinase |
| CCND2 | P30279 | G1/S-specific cyclin-D2 |
| EPHA3 | P29320 | Ephrin type-A receptor 3 |
| CD38 | P28907 | ADP-ribosyl cyclase/cyclic ADP-ribose hydrolase 1 |
| CTSS | P25774 | Cathepsin S |
| CXCR1 | P25024 | C-X-C chemokine receptor type 1 |
| TBXAS1 | P24557 | Thromboxane-A synthase |
| KCNA5 | P22460 | Potassium voltage-gated channel subfamily A member 5 |
| ERBB3 | P21860 | Receptor tyrosine-protein kinase erbB-3 |
| Continued | | |

| Symbol | Uniprot | Protein name |
|---|---|---|
| CXCL2 | P19875 | C-X-C motif chemokine 2 |
| ALOX12 | P18054 | Polyunsaturated fatty acid lipoxygenase ALOX12 |
| IGFBP3 | P17936 | Insulin-like growth factor-binding protein 3 |
| GJA1 | P17302 | Gap junction alpha-1 protein |
| PECAM1 | P16284 | Platelet endothelial cell adhesion molecule |
| CBR1 | P16152 | Carbonyl reductase |
| ST6GAL1 | P15907 | Beta-galactoside alpha-2,6-sialyltransferase 1 |
| MMP9 | P14780 | Matrix metalloproteinase-9 |
| TYR | P14679 | Tyrosinase |
| NCF1 | P14598 | Neutrophil cytosol factor 1 |
| SELL | P14151 | L-selectin |
| MAP2 | P11137 | Microtubule-associated protein 2 |
| MAPT | P10636 | Microtubule-associated protein tau |
| SPP1 | P10451 | Osteopontin |
| CXCL8 | P10145 | Interleukin-8 |
| FBP1 | P09467 | Fructose-1,6-bisphosphatase 1 |
| PTPRC | P08575 | Receptor-type tyrosine-protein phosphatase C |
| GSTA1 | P08263 | Glutathione S-transferase A1 |
| MMP3 | P08254 | Stromelysin-1 |
| RET | P07949 | Proto-oncogene tyrosine-protein kinase receptor Ret |
| ADRB2 | P07550 | Beta-2 adrenergic receptor |
| BCHE | P06276 | Cholinesterase |
| IL6 | P05231 | Interleukin-6 |
| MPO | P05164 | Myeloperoxidase |
| ARG1 | P05089 | Arginase-1 |
| ERBB2 | P04626 | Receptor tyrosine-protein kinase erbB-2 |
| MMP1 | P03956 | Interstitial collagenase |
| CRYAB | P02511 | Alpha-crystallin B chain |
| IL1B | P01584 | Interleukin-1 beta |
| MYC | P01106 | Myc proto-oncogene protein |
| AKR1B10 | O60218 | Aldo–keto reductase family 1 member B10 |
| MGAM | O43451 | Maltase-glucoamylase, intestinal |
| CYP27B1 | O15528 | 25-hydroxyvitamin D-1 alpha hydroxylase, mitochondrial |
| PTGES | O14684 | Prostaglandin E synthase |

**Table 2.** Information on 90 crossed target genes.

molecules are located in the corresponding docking pockets, forming hydrogen bonds between receptors and ligands, confirming the high accuracy of drug target prediction in this study from the perspective of molecular docking. The compound-target interactions with the free binding energy scores along with their binding mode were determined using PyMoL-2.3. (Supplementary Fig. S3). Figure 8 illustrates MMP9 and their ligand's local structures of molecular docking in detail. The free binding energy of compound with MMP9 (PDB id-2OW0) was luteolin (− 10.7 kcal/mol). The binding affinity was contributed the hydrogen bonding with the ALA-189, GLN-402, LEU-188, TYR-420. The free binding energy of compound with IL6 (PDB id- 1ALU) was luteolin (− 7.2 kcal/mol). The amino acids corresponding to the bonded hydrogen bonds are ARG-179, GLN-175 residues. And the best compound's binding affinity with MPO (PDB id- 1D2V) was quercetin (− 7.9 kcal/mol), the bonded hydrogen bonding with ARG-424, ARG-333, HIS-336 residues. IL1B's (PDB id- 1L2H) best ingredient's binding affinity was quercetin (− 7.5 kcal/mol) and bonded hydrogen bonding was ASN-7, LYS-65 residues.

## Discussion

The modern research of traditional Chinese medicine (TCM) entered a new period, using science and technology combined with traditional Chinese medicine theory, the network medicine pharmacology aims to clarify the research method of traditional Chinese medicine effective component and targets in the system of the molecular level to better understand and predict the behavior of cells, tissues or organs of the body function of phenotypic effects which provides a new perspective method to analyze drug effects. The research mode of "one drug, one target" is transformed into the research concept of "multiple approaches and multiple targets"[41]. Different from the fixed pathogenic genes in the previous disease database, the screening of pathogenic genes in GEO database provides more possibilities for the prediction of disease targets in network pharmacology, and become more conducive to the mining of drug targets and possible pharmacological mechanisms. However, there are still a
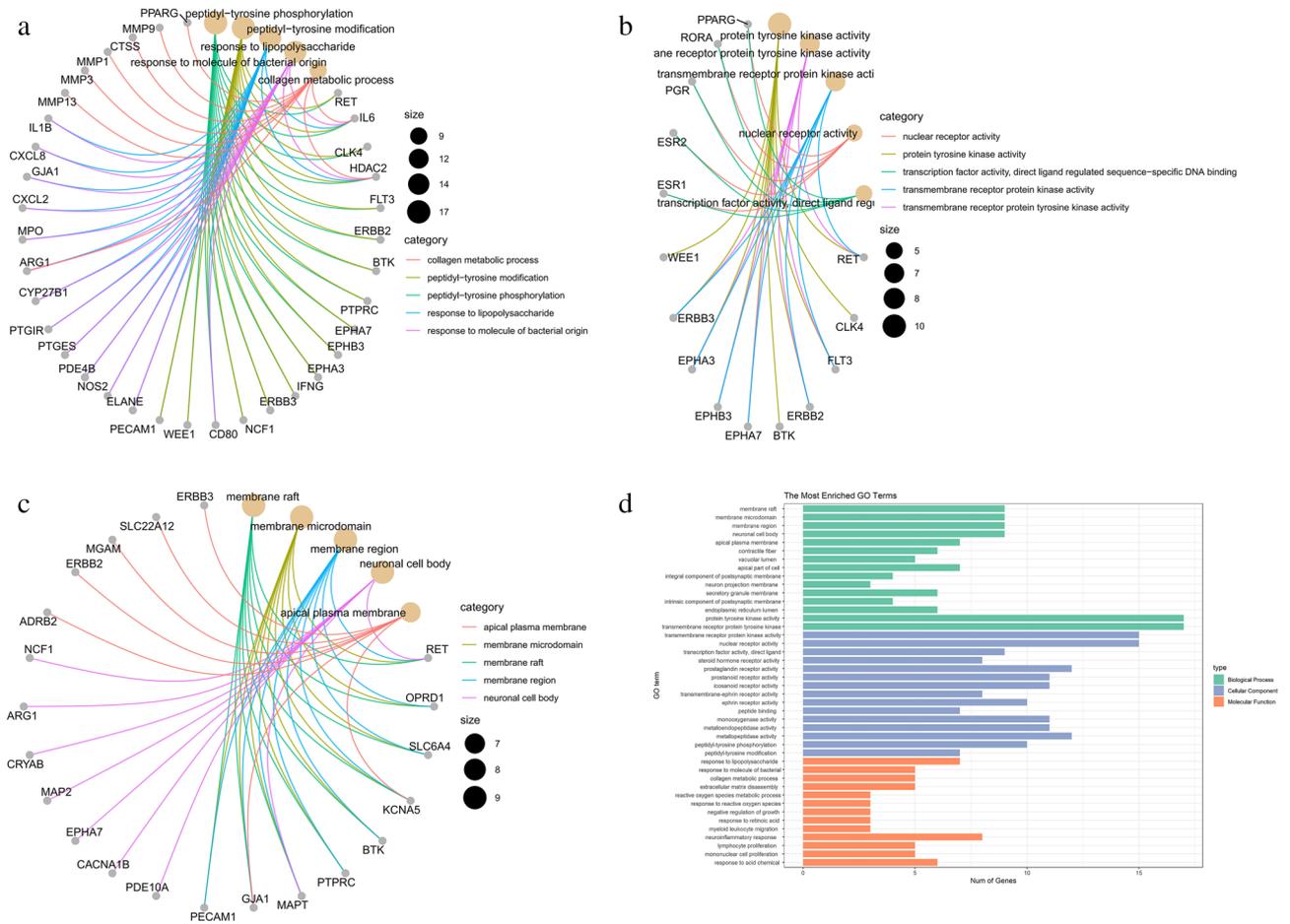
**Figure 4.** GO enrichment analysis of the anti-Peri-implants targets of PCRER. (**a**) Biological processes; (**b**) molecular function; (**c**) cellular components; (**d**) the 15 most enriched GO terms.
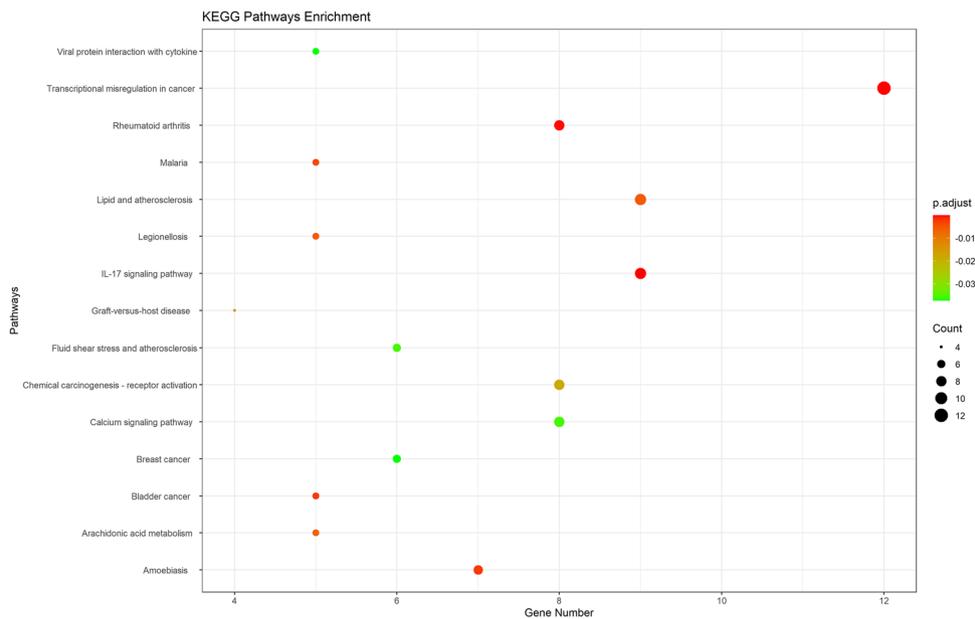


**Figure 5.** KEGG pathway enrichment analysis of the anti-Peri-implants targets of PCRER.

lot of progress spaces in this discipline. For example, how many false positive rates do we have after discovering possible therapeutic targets of drugs, and how accurate is the verification through machine learning such
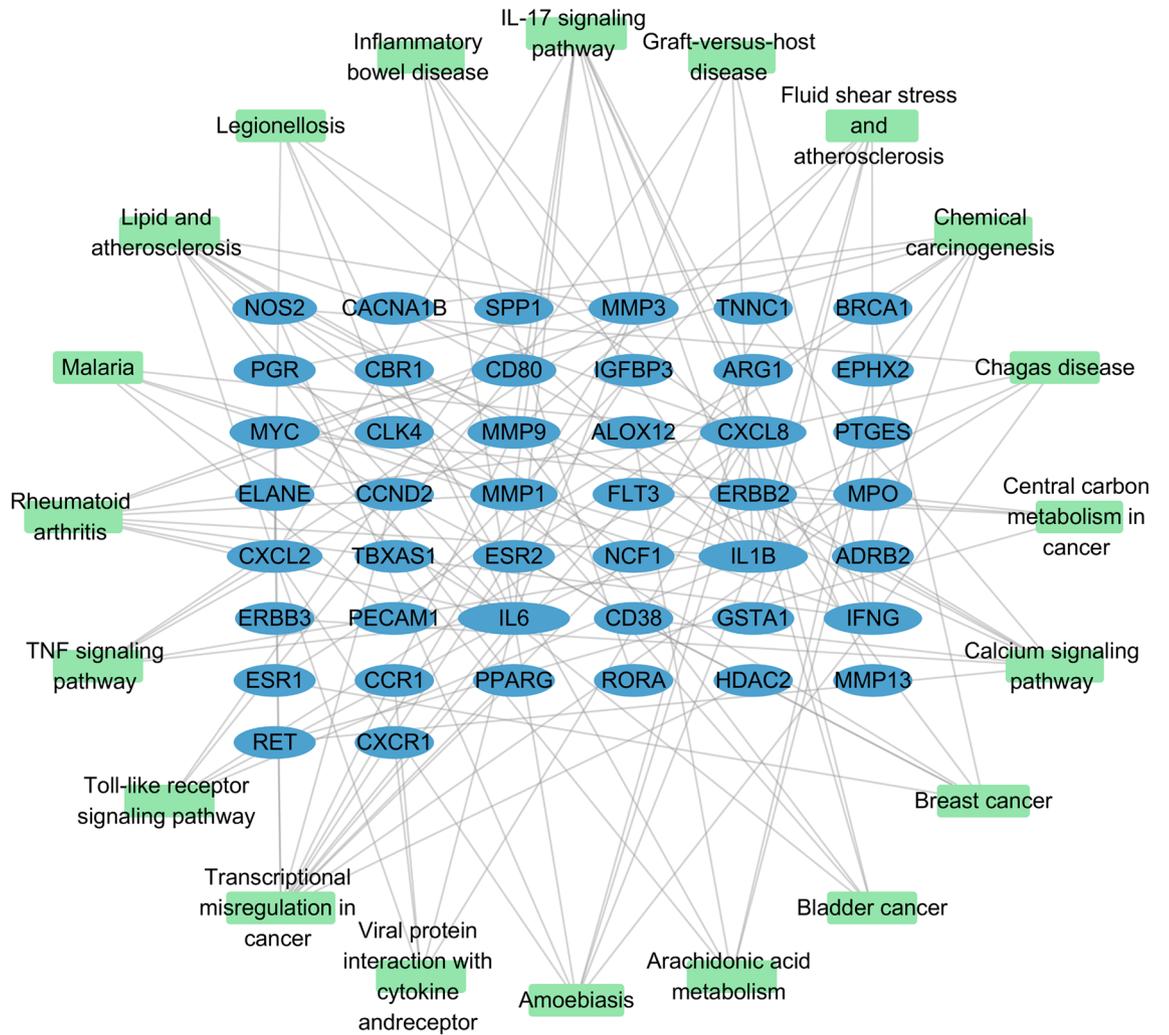
**Figure 6.** The target–pathway network implicated in the mechanism of PCRER in Peri-implants treatment. The green nodes represent the pathways, represent the interaction between the pathways and the targets, whereas the lake blue nodes represent the targets involved in these pathways is proportional to the degree of interaction.
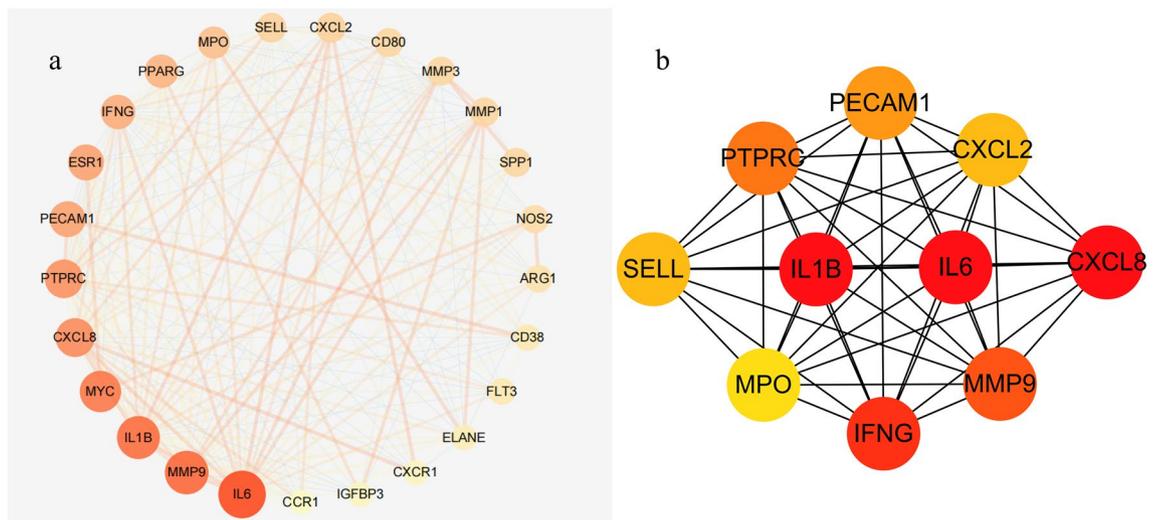


**Figure 7.** Protein–protein interaction network. (**a**) PPI network of target genes using MCODEm (**b**) subnetwork of top nine hub using CytoHubba. Node color reflects the degree of connectivity (red color represents a higher degree, and yellow color represents a lower degree).

| Ligands | Protein | PDB ID | RMSD (Å) | Free binding energy (kcal/mol) |
|---|---|---|---|---|
| Picralinal | MMP9 | 2OW0 | 2.00 | − 8.3 |
| Physciondiglucoside | MMP9 | 2OW0 | 2.00 | − 8.1 |
| Rhein | MMP9 | 2OW0 | 2.00 | − 9.9 |
| Torachrysone-8-O-beta-D-glucoside | MMP9 | 2OW0 | 2.00 | − 8.6 |
| Luteolin | MMP9 | 2OW0 | 2.00 | − 10.7 |
| Quercetin | MMP9 | 2OW0 | 2.00 | − 10.5 |
| Resveratrol | MMP9 | 2OW0 | 2.00 | − 9.2 |
| Polydatin | MMP9 | 2OW0 | 2.00 | − 9.9 |
| Emodin | MMP9 | 2OW0 | 2.00 | − 9.5 |
| 6,8-Dihydroxy-7-methoxyxanthone | IL6 | 1ALU | 1.90 | − 6.2 |
| Physciondiglucoside | IL6 | 1ALU | 1.90 | − 6.1 |
| Torachrysone-8-O-beta-D-glucoside | IL6 | 1ALU | 1.90 | − 6.0 |
| Luteolin | IL6 | 1ALU | 1.90 | − 7.2 |
| Quercetin | IL6 | 1ALU | 1.90 | − 6.9 |
| Resveratrol | IL6 | 1ALU | 1.90 | − 6.2 |
| Luteolin | MPO | 1D2V | 1.75Å | − 7.9 |
| Quercetin | MPO | 1D2V | 1.75Å | − 7.9 |
| Resveratrol | MPO | 1D2V | 1.75Å | − 7.5 |
| Quercetin | IL1B | 1L2H | 2.00 | − 7.5 |
| Resveratrol | IL1B | 1L2H | 2.00 | − 6.0 |
| Emodin | IL1B | 1L2H | 2.00 | − 7.3 |
| Rhein | SELL | 3CFW | 2.20 | − 7.1 |
| Polydatin | SELL | 3CFW | 2.20 | − 6.8 |
| Luteolin | IFNG | 1FYH | 2.04 | − 7.9 |
| Quercetin | IFNG | 1FYH | 2.04 | − 8.0 |
| Quercetin | CXCL8 | 1ICW | 2.01 | − 6.2 |
| Resveratrol | CXCL8 | 1ICW | 2.01 | − 5.5 |
| Quercetin | CXCL2 | 5OB5 | 1.65 | − 8.7 |
| Rhein | PTPRC | 1YGR | 2.90 | − 7.0 |
| Resveratrol | PECAM1 | 5C14 | 2.80 | − 6.1 |

**Table 3.** Free binding energy of nine hub genes with their corresponding active compounds.

as molecular docking and depth algorithm? This needs to be confirmed by subsequent dry and wet tests[42]. As a common inflammatory disease that affects the life span of implants, the incidence rate of Peri-implants is increasing yearly and has seriously affected human health, especially the elderly[8]. At present, non-steroidal drugs are mainly used to treat it. PCRER and its main components have limited targets and pathways, most of which were obtained through preliminary tests or literature review. Therefore, we aim to explore the molecular mechanism of PCRER in the treatment of peri-implantitis by using big data mining and network pharmacology methods.

Due to the lack of corresponding disease target data in Peri-implants, we combined GEO database to conduct network pharmacology analysis which was also the first article about Peri-implants combined with network drugs. We used TCMSP database to identify the active components of PCRER. A total of 13 core active components were identified. Among them, beta-sitosterol, Luteolin, Quercetin and Resveratrol can match more than 20 targets. The pathogenesis of Peri-implants was complex and believed to be caused by a series of interactions such as inflammation, oxidative stress and bacterial infection. The osteoprotective effect of Quercetin has been confirmed by a large number of in vitro and in vivo experiments. Studies have reported the activation of Quercetin on osteoblast formation, as well as stimulating matrix mineralization, calcium deposition, and the expression of ALP, COL1, RUNx-2 and other osteogenic genes[43,44]. Yu Wei et al. found that quercetin increased the antioxidant capacity of PDLCs by activating NRF2 signaling pathway, alleviated oxidative stress damage, and alleviated alveolar bone loss in periodontitis[45]. Luteolin, flavonoid plant, has potent anti-inflammatory effects both in vitro and in vivo that can effectively inhibit the production of TNF-α, IL-6 and NO in LPS induced macrophage-like cell lines, and luteolin's inhibition of inflammatory cytokines and/or ROS production may lead to the inhibition of osteoclast differentiation[46]. Kim found that luteolin also reduced the absorption activity of mature osteoclasts. In addition, it prevented the loss of bone mass, especially trabecular bone that occur after ovaries removal by inhibiting bone turnover[47]. In the experiment of luteolin, Hatice found that luteolin significantly reduced alveolar bone loss by decreasing MMP-8 and RANKL expression, increasing osteoblast activity and upregulation of TIMP-1, BMP-2 and OPG expression[48]. Resveratrol can inhibit the expression of Toll-like receptor (TLR) and pro-inflammatory genes, activate Sirt1 and then inhibit the expression of inflammatory factors such as TNF-α, IL-1, IL-6, MMP-1, MMP3 and COX-2 induced by NF-KB, and play a double blocking role in NF-KB signaling pathway[49]. In addition, resveratrol regulates immunity by interfering with immune cell regulation,
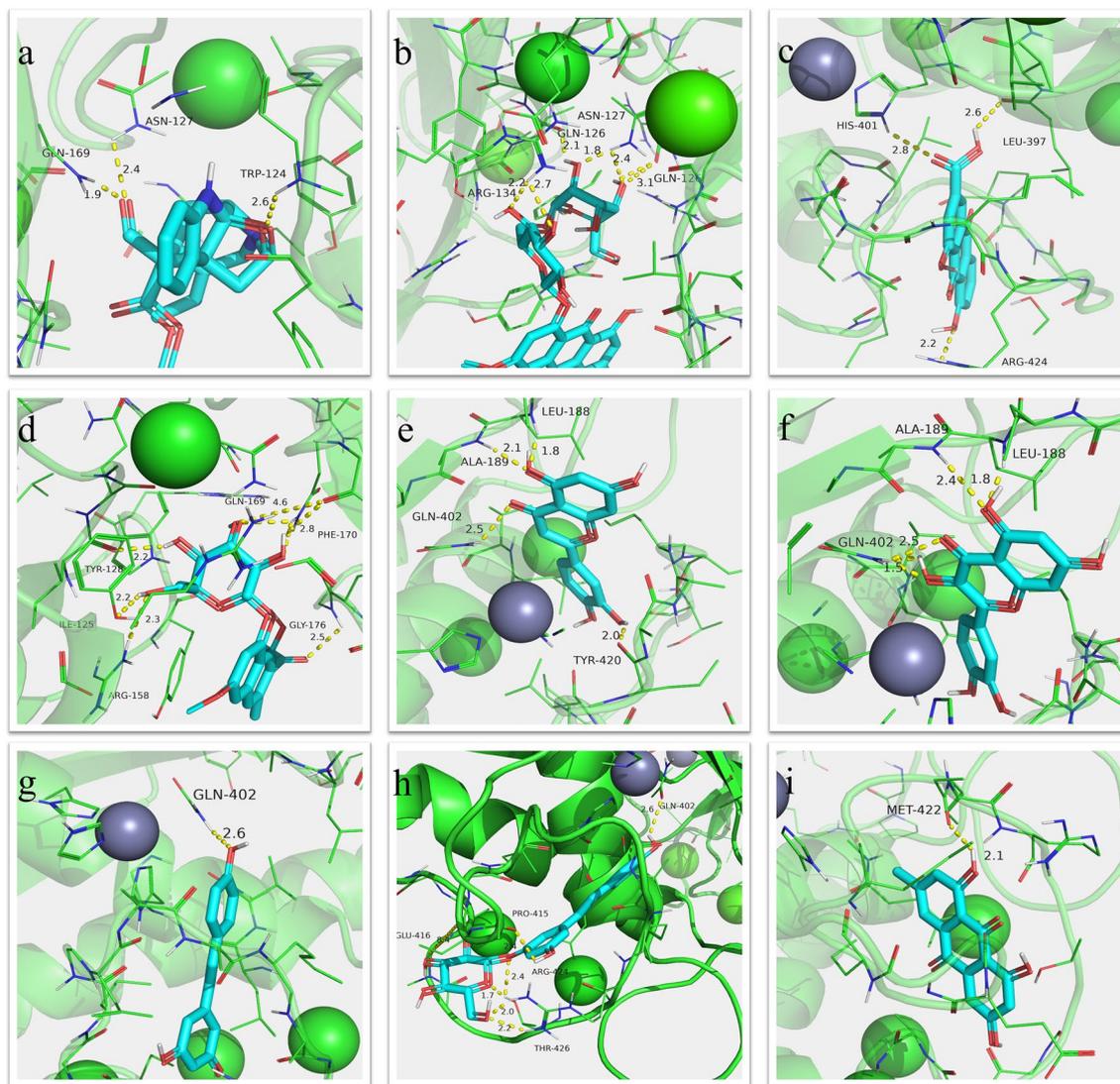
**Figure 8.** The highest bind affinity compounds in Nine hub genes of molecular docking. (**a**) MMP9-Picralinal; (**b**) MMP9-Physciondiglucoside; (**c**) MMP9-rhein; (**d**) MMP9- Torachrysone-8-O-beta-D-glucoside; (**e**) MMP9-luteolin; (**f**) MMP9-quercetin; (**g**) MMP9- resveratrol; (**h**) MMP9-polydatin; (**i**) MMP9-emodin (PyMoL-2.3 https://pymol.org/dokuwiki/?id=media:new23).

proinflammatory cytokine synthesis and gene expression and plays a beneficial role in the prevention of chronic diseases related to inflammation. Resveratrol has also been proved to inhibit osteoclast differentiation and induce bone formation potential. Ribeiro found resveratrol could improve bone repair around titanium implants in rats, reverse the negative effects of implants and reduce the expression of RANKL/OPG in peri-implant tissues during bone repair[50]. Hua Y's study found that resveratrol treatment could improve osseointegration of implants and promote bone formation by reducing bone loss damage caused by AGE's deposition[23]. Therefore, resveratrol may be the key component of polygonum cuspidate in the treatment of peri-implantitis.

According to the active ingredients of the drugs mentioned above, we used related database to screen the putative targets and obtained 930 targets of PCRER. Then, we integrated three gene microarray chips of GEO, finally obtaining 1399 disease target genes. Peri-implants is a chronic inflammatory disease associated with a variety of inflammation pathways and cell phenotypes. To explore the PCRER 's potential mechanism, we conducted GO and KEGG enrichment analysis to explore possible regulating network. The results showed that the mapped targets were enriched to 29 items in biological process, which were mainly related to the regulation of membrane function included raft, microdomain, region, organelle outer membrane and caveola among others. It also enriched to 51 items in the cell composition, 13 items in biological process, and 328 terms in molecular functions. In addition, we observed 20 KEGG pathways related to Peri-implants and constructed a "Targets-Pathways" network, which involved IL-17 signaling pathway, Calcium signaling pathway, Toll-like receptor signaling pathway, TNF signaling pathway. IL-17 signaling pathway plays an important role in maintaining the balance between Th17 cells and Treg cells, promoting the differentiation of Th17 cells and the secretion of IL-17, triggering the immune response of the body, thus activating osteoclasts and secreting MMP to cause the degradation of type II collagen[51]. There is evidence that IL-17 is involved in the pathogenesis of periodontal diseases, and

the level of IL-17 in peri-implant sulcular fluid (PISF) increases during peri-implant inflammation[52]. Calcium ($Ca^{2+}$) is essential for bone homeostasis. $Ca^{2+}$ signaling regulates proliferation, differentiation and apoptosis of osteocytes. RANKL induces $Ca^{2+}$ signaling in osteoclasts through calmodulin. $Ca^{2+}$ could bind to CaM and stimulates $Ca^{2+}$/ CAM-dependent kinase (CaMK) and calcineurin, leading to induction and activation of NFATc1 and (PGC1β). PGC1β regulates mitochondrial biogenesis and plays an important role in the terminal differentiation of osteoclasts[53,54]. As mentioned above, T cell signaling pathways are hypothesized to be key mediators of persistent infection-induced chronic inflammatory processes in periodontitis and periapical periodontitis which is also influenced by $Ca^{2+}$ signaling pathways and $Ca^{2+}$ channel regulation. With advances in the study of $Ca^{2+}$ signaling pathways in T cell pathogenicity and homeostasis, oral barrier immune cells may be affected by CCB and may lead to inflammatory gingival enlargement[55]. As you can imagine, the susceptibility of periodontitis or Peri-implants are directly related to calcium signaling or dysfunction. Toll-like receptor (TLR) is a class of pattern recognition receptors that can recognize microbial components. LPS can interact with TLR2, a major member of the TLR family, to activate the downstream protein nuclear factor-κB (NF-κB), P38 mitogen-activated protein kinase (MAPK) and C-Jun N-terminal kinase (JNK) of TLR2 and regulate the production of LPS-induced pro-inflammatory cytokines such as IL6[56]. TLR2 initiates intracellular signaling cascades through cytoplasmic intermediates including Myd88, ultimately leading to activation of NF-κB and MAPK, thereby enhance transcription of inflammatory cytokines. A recent study also confirmed that TLR2 signaling activation plays a key role in bone loss and increased inflammatory infiltration in peri-implant inflammation[57]. Therefore, inhibition of TLR2 signal activation may be an effective strategy for the treatment of Peri-implants. Currently, TNF-α was considered to mediate bone resorption mainly by promoting osteoclast differentiation and inhibiting osteoblast differentiation[58]. Darabi found that TNF-α content was positively correlated with periodontal depth (PD)[59]. The increase of PD suggested that the binding between implant and surrounding tissue was damaged, and the degree of inflammation around implant increased, indicating that TNF-α expression level was closely related to the severity of implant inflammation and could indirectly reflect the health status of surrounding tissue[60]. TNF-α promoted osteoclast synthesis, reduced bone matrix calcification and promoted bone resorption, so it was speculated that TNF-α may be involved in the reconstruction of implant bone tissue.

In this study, STRING database was used to calculate the degree of PCRER anti-Peri-implants targets (90 genes), MCODE and CytoHubba plug-in in Cytoscape software was used for screening the top 10 hub genes (MMP9, IL6, MPO, IL1B, SELL, IFNG, CXCL8, CXCL2, PTPRC, PECAM1). MMP-9 ,an inflammatory marker of peri-implant inflammation, mainly present in oral fluid and inflamed gingival tissue in this specimen[61] and primarily secreted by neutrophils and macrophages, regulates inflammation in tissues and diseases[62]. MMP9's expression is significantly increased in chronic periapical infection area and overexpression of MMP-9 attenuates osteoclast formation and inhibits secretion of pro-inflammatory cytokines[63]. MMP9 initiates osteoclasts by removing collagen from demineralized bone, which is essential[64]. Shimada found that titanium stimulated the expression of MMP-9 mRNA in osteoblasts cultured in vitro, and zirconia inhibited the expression of MMP-9 mRNA[65]. Meanwhile, Degidi et al. also confirmed that the level of MMP9 around the healing cap was increased[66]. However, more research is needed on the regulatory mechanism of MMP-9.

Peri-implants is mainly caused by bacterial infection of the implant-confined tissues and the destruction of the soft tissue closure of the cuff of the implant. As a result, the inflammation of the body tissues is the result of the interaction between the pathogenic agent and the immune system of the host. Cytokines are involved in the inflammation and immune response of the body. IL-1β is closely associated with implant inflammation around the important inflammatory factor which inhibits the expression of alkaline phosphatase, coordinates to polyclonal activators to stimulate proliferation of T cells and B cells growth and differentiation[67], regulates immune response, stimulates the mononuclear macrophage and produce IL-6, which can increase the activity of osteoclast. At the same time, IL-1 can also inhibit the synthesis of osteoblast calcium cord and destroy normal bone metabolism, so it is called osteoclast activating factor[68]. In addition, IL-1β also interact with other inflammatory mediators, promotes the expression of cytokines such as IL-6, TNF-α and intercellular adhesion molecules, and cascades the inflammatory effect to amplify the inflammatory response, resulting in aggravated tissue damage[69]. Studies have shown that the expression level of IL-1β at peri-implantitis sites was significantly higher than healthy implant sites. IL-6 is produced by mononuclear macrophages under the induction of IL-1. The level of IL-6 is related to the active stage of the disease, which is consistent with the detection results of gingival crevicular fluid in patients with periodontal disease. IL-6 stimulates the growth and differentiation of osteoclast precursors. Promoting alveolar bone absorption which is thought to amplify the biological effects of IL-1[70]. Sakai et al. found that IL-1β concentration was correlated with bone tissue absorption around implants, which could be used as a sensitive indicator to detect bone absorption at peri-implant inflammatory edge[70]. These results suggest that the pro-inflammatory cytokine IL-1β was involved in the occurrence and development of peri-implant inflammation, which could be used to distinguish the peri-implant health from the inflammatory state and a standard tool for the evaluation of peri-implant tissue health and treatment of Peri-implants.

Among cytokines regulating bone metabolism, interferon G (IFNG) has been shown to play an important role in the regulation of osteoporosis. In vitro, IFNG inhibit osteoclast formation by stimulating bone marrow monocyte precursors with receptor-activated nuclear factor-κB ligand (RANKL)[71]. However, IFNG is more complex in vivo, in cell culture, IFNG can inhibit the function of osteoblasts and effectively inhibit the formation of osteoclasts. In bone explants, it inhibits osteoclast differentiation[72]. IFNG together with interleukin 1 (IL-1) stimulates high levels of NO production in bone, and these early studies support the role of IFNG in bone formation[73]. In addition, IFNG induces the expression of Best5 gene expressed during bone formation in rats[74]. Gustavo found that the addition of low doses of IFNG in ovariectomized mice reversed the phenotype of previous osteoporosis, which proved that the beneficial effect of low doses of IFNG on bone formation, and IFNG's effect on bone resorption was dominant[75]. Although the role of IFNG in osteoclast differentiation and activity has been extensively studied, little is known about its role in periodontitis and peri-implants. However, it remains

to be determined whether IFNG indirectly regulates osteoclast activity mainly through RANKL expression in osteoblasts. Chemokines are proteins (such as IL-8, MCP-1, CXCL2, etc.) with low molecular weight (usually 8-10kD) that attract white blood cells to migrate to the site of infection and play an important role in inflammatory response. CxCL8/IL-8 could induce neutrophils to produce chondrodegrading enzymes, resulting in joint tissue damage. Elevated IL-8 levels often associated with locally infiltrated monocytes and neutrophils[76]. CXCL2 as a subtype of chemokine, has been widely expressed in RANKL-induced osteoclast precursor cells and plays an important role in the formation, migration and differentiation of osteoclasts. The study of Ha et al. showed that RANKL could promote CXCL2 expression of osteoclasts in vitro, so as to enhance their proliferation and differentiation ability, which might have a positive effect on bone resorption. Thus, CXCL2 is indeed closely associated with bone remodeling[77]. Previous studies by Gamonal et al. found that the level of IL-8 in the gingival of patients with periodontitis was higher than that of healthy subjects, but decreased significantly after periodontal treatment, suggested that IL-8 was involved in the inflammatory process of periodontitis[78]. Pietruski et al. observed that IL-8 level in gingival crevicular fluid increased significantly 24 h after implant implantation, indicated that there was local inflammation on the day after surgery, and surgical trauma inevitably led to regeneration and repair of local body tissues and IL-8 level decreased 4 months after surgery[79].

Myeloperoxidase (MPO), the most abundant protein in neutrophils which is a powerful oxidant and is involved in defense mechanisms against infectious agents; However, when it is uncontrollable or over-activated, it can act on host cells and inactivate humoral factors[80]. Liskmann et al. concluded that elevated MPO levels were associated with detecting bleeding and pocket depth around diseased and healthy implants in the same individual. Specifically, it was found that only 9.4% of healthy implants had MPO levels above 25 ng/mg, while 96.9% of diseased implants had MPO levels above 25 ng/mg[81], Montero found that the level of Myeloperoxidase was in direct proportion to the risk of peri-implants in beagles (odds ratio: 1.1)[82]. Quantitative measurement of MPO can be used as an adjunct to traditional clinical parameters[83]. SELL (Lymphocyte homing receptor) belongs to the lymphocyte homing receptor (LHR) family, which is one of the family members of cell adhesion molecules. SELL is involved in cell extension and movement, cell signal transduction and inflammatory response, immune response, thrombosis, wound healing and other physiological and pathological processes[84]. Seidelin et al.[85] showed that the serum SL-selectin level of patients with severe infectious diseases was significantly higher than that of normal people. Asami et al. also screened SELL as its hub gene after bioinformatics analysis of the GEO database of periodontitis[86], but there is still a lack of basic research on this gene in periodontitis and peri-implantitis.

Platelet endothelial cell adhesion molecule-1 (PECAM1), also known as CD31, is a type I transmembrane adhesion protein, it has been shown that inhibition of PECAM1 can reduce inflammatory responses in various human diseases, such as arthritis[87] and atherosclerosis[88]. A previous report by Cheng et al.[89] suggested that PECAM1 was critical in the inflammatory response and apoptosis of hepatitis liver. Meanwhile, Liu et al. found that PECAM1 could interact with CXCR4 in experimental pulpitis in mice, which lead to inflammatory response and increased apoptosis of human pulp fibroblasts by activating the NF-KB signaling pathway[90]. Wu found that PECAM-1 was found to be a negative regulator of monocyte derived osteoclast formation in PECAM-1 knockout mice[91]. Therefore, we speculate that PECAM-1's deficiency may have a direct and significant effect on osteoclast formation and indirectly affect osteoblast function. PTPRC encodes protein Tyrosine Phosphatase (PTP), a signaling molecule known as CD45 that regulates a variety of cellular processes and plays a key role in the immune system[92]. In addition, PTPRC can negatively regulate cytokine receptor signaling by inhibiting JAK signaling[93]. PECAM-1 and PTPRC have not been reported in relation to periodontitis or peri-implantitis. It is worth noting that molecular docking simulation is an important method for structural molecular biology and computer-aided drug design, and the results of molecular docking also show that PCRER's components have good binding performance with the Hub genes.

In this study, network pharmacology and molecular docking methods were used to predict the mechanism of PCRER in the treatment of peri-implantitis. At the same time, the direct intersection targets were analyzed by GO annotation and KEGG enrichment, and the Hub targets were screened from the direct targets by PPI network and Cytoscape intersection analysis, revealing the possible physiological and pathological process of PCRER intervention in peri-implantitis. At the same time, because the traditional Chinese medicine may play a role in treating diseases through the synergistic effect of multiple components, how to predict and evaluate the synergistic effect of multiple compounds become a challenge we are facing at present. As for the limitations of this paper and aspects that need further study, first of all, we can use liquid chromatography-mass spectrometry to verify and supplement the effective compounds of PCRER, animal and cell experiments and clinical samples were also needed to detect the corresponding gene and pathway levels and conduct corresponding pharmacokinetic and metabonomics studies[42]. In terms of data collection, the current prediction platform lacks information on active ingredient activation or inhibition targets and signaling pathways, which is the deficiency of this paper. If we can constantly improve the above shortcomings, we will be able to provide more reliable theoretical basis for the study of traditional Chinese medicine.

## Conclusion

In summary, the potential molecular mechanism and target gene of PCRER treat Peri-implants were elucidated by network pharmacology method that beta-sitosterol, luteolin, quercetin, resveratrol could be the vital ingredients for PCRER. PCRER's core components are expected to be effective drugs to treat Peri-implants by anti-inflammation, promotes bone metabolism. However, whether it is suitable for long-term maintenance treatment of Peri-implants still needs to be determined according to the future basic experiments. In addition, clinical trials are needed to elucidate the mechanism of action.

## Data availability

All data in this paper can be collated from the open source website provided by us and analyzed by relevant software.

## References

1. Silva, R. C. E. & Reis, M. B. L. Association between genetic polymorphisms in RANK, RANKL and OPG and Peri-Implant diseases in patients from the Amazon. *Region* **31**(1), 63–68 (2020).
2. Matys, J., Botzenhart, U., Gedrange, T. & Dominiak, M. Thermodynamic effects after Diode and Er:YAG laser irradiation of grade IV and V titanium implants placed in bone—An ex vivo study Preliminary report. *Biomedizinische Technik Biomed. Eng.* **61**(5), 499–507 (2016).
3. Salvi, G. E., Cosgarea, R. & Sculean, A. Prevalence of Periimplant diseases. *J. Appl. Oral Sci. Revista FOB* **28**(2), 100–102 (2019).
4. Kormas, I., Pedercini, C., Raptopoulos, M., Alassy, H. & Wolff, L. F. Peri-Implant diseases: Diagnosis, clinical, histological, micro-biological characteristics and treatment strategies. A narrative review. *Antibiotics (Basel, Switzerland)* **9**(11), 835 (2020).
5. Barootchi, S., Ravidà, A., Tavelli, L. & Wang, H. L. Nonsurgical treatment for peri-implant mucositis: A systematic review and meta-analysis. *Int. J. Oral Implantol. (Berlin, Germany)* **13**(2), 123–139 (2020).
6. Heo, S., Kim, H. J., Lee, J. & Kim, S. J. Simplified nonsurgical treatment of peri-implantitis using chlorhexidine and minocycline hydrochloride. *J. Periodontal Implant Sci.* **48**(5), 326–333 (2018).
7. Ramos, U. D. *et al.* Comparison between two antimicrobial protocols with or without guided bone regeneration in the treatment of peri-implantitis. A histomorphometric study in dogs. *Clin. Oral Implants Res.* **28**(11), 1388–1395 (2017).
8. Kwon, T., Wang, C. W., Salem, D. M. & Levin, L. Nonsurgical and surgical management of biologic complications around dental implants: Peri-implant mucositis and peri-implantitis. *Quintessence Int. (Berlin, Germany: 1985)* **51**(10), 810–820 (2020).
9. Wang, Y., Yang, H., Chen, L., Jafari, M. & Tang, J. Network-based modeling of herb combinations in traditional Chinese medicine. *Brief. Bioinform.* https://doi.org/10.1093/bib/bbab106 (2021).
10. Li, Y.-Q. *et al.* Integrated network pharmacology and zebrafish model to investigate dual-effects components of *Cistanche tubulosa* for treating both Osteoporosis and Alzheimer's Disease. *J. Ethnopharmacol.* **254**, 112764 (2020).
11. Kohl, S. European Directorate for the Quality of Medicines: automatic drugs dispensing report. *Eur. J. Hosp. Pharm. Sci. Pract.* **25**(3), 169–172 (2018).
12. Na, Y. Clinical effect of *Polygonum cuspidatum* Tongfeng Decoction on gouty arthritis. *Cardiovasc. Dis. Electron. J. Integr. Traditi. Chin. West. Med.* **7**(25), 162–163 (2019).
13. Run mei Wang, J. B. X. Clinical application of *Polygonum cuspidatum*. *Chin. J. Ethnomed. Ethnophammcy* **16**, 52 (2011).
14. Tongyue, H. M. W. R. Z. X. Y. A study on the clinical application and dosage of giant knotweed rhizome. *Jilin J. Chin. Med.* **41**(12), 1657–1660 (2021).
15. Lim, B. O. *et al.* Polygoni cuspidati radix inhibits the activation of Syk kinase in mast cells for antiallergic activity. *Exp. Biol. Med. (Maywood, NJ)* **232**(11), 1425–1431 (2007).
16. Liu, Z. P. *et al.* Effects of trans-resveratrol from *Polygonum cuspidatum* on bone loss using the ovariectomized rat model. *J. Med. Food* **8**(1), 14–19 (2005).
17. Song, J. H. *et al.* In vitro inhibitory effects of *Polygonum cuspidatum* on bacterial viability and virulence factors of Streptococcus mutans and Streptococcus sobrinus. *Arch. Oral Biol.* **51**(12), 1131–1140 (2006).
18. Ban, S. H. *et al.* Effects of a bio-assay guided fraction from *Polygonum cuspidatum* root on the viability, acid production and glucosyltranferase of mutans streptococci. *Fitoterapia* **81**(1), 30–34 (2010).
19. Nawrot-Hadzik, I. *et al.* Chemical composition of East Asian invasive knotweeds, their cytotoxicity and antimicrobial efficacy against cariogenic pathogens: An in-vitro study. *Med. Sci. Monit.* **25**, 3279–3287 (2019).
20. Li, H., Chen, Z., Zhong, X., Li, J. & Li, W. Mangiferin alleviates experimental peri-implantitis via suppressing interleukin-6 production and Toll-like receptor 2 signaling pathway. *J. Orthop. Surg. Res.* **14**(1), 325 (2019).
21. Galarraga-Vinueza, M. E. *et al.* Anti-inflammatory and macrophage polarization effects of Cranberry Proanthocyanidins (PACs) for periodontal and peri-implant disease therapy. *J. Periodontal Res.* **55**(6), 821–829 (2020).
22. Wong, S. K., Chin, K. Y. & Ima-Nirwana, S. Quercetin as an agent for protecting the bone: A review of the current evidence. *Int. J. Mol. Sci.* **21**(17), 6448 (2020).
23. Hua, Y., Bi, R., Li, Z. & Li, Y. Resveratrol treatment promotes titanium implant osseointegration in diabetes mellitus rats. *J. Orthop. Res.* **38**(10), 2113–2119 (2020).
24. Li, S. *et al.* Understanding ZHENG in traditional Chinese medicine in the context of neuro-endocrine-immune network. *IET Syst. Biol.* **1**(1), 51–60 (2007).
25. Zhang, R., Zhu, X., Bai, H. & Ning, K. Network pharmacology databases for traditional Chinese medicine: Review and assessment. *Front. Pharmacol.* **10**, 123 (2019).
26. Xie, W. *et al.* Panax Notoginseng Saponins: A review of its mechanisms of antidepressant or anxiolytic effects and network analysis on phytochemistry and pharmacology. *Molecules (Basel, Switzerland)* **23**(4), 940 (2018).
27. Tao, W. *et al.* Network pharmacology-based prediction of the active ingredients and potential targets of Chinese herbal Radix Curcumae formula for application to cardiovascular disease. *J. Ethnopharmacol.* **145**(1), 1–10 (2013).
28. Wang, X., Wang, Z.-Y., Zheng, J.-H. & Li, S. TCM network pharmacology: A new trend towards combining computational, experimental and clinical approaches. *Chin. J. Nat. Med.* **19**(1), 1–11 (2021).
29. Ru, J. *et al.* TCMSP: A database of systems pharmacology for drug discovery from herbal medicines. *J. Cheminform.* **6**, 13 (2014).
30. Huang, J. *et al.* Identification of the active compounds and significant pathways of yinchenhao decoction based on network pharmacology. *Mol. Med. Rep.* **16**(4), 4583–4592 (2017).
31. Gfeller, D. *et al.* SwissTargetPrediction: A web server for target prediction of bioactive small molecules. *Nucleic Acids Res.* **42**(W1), W32–W38 (2014).
32. Keiser, M. J. *et al.* Relating protein pharmacology by ligand chemistry. *Nat. Biotechnol.* **25**(2), 197–206 (2007).
33. Gajjar, N. D., Dhameliya, T. M. & Shah, G. B. In search of RdRp and Mpro inhibitors against SARS CoV-2: Molecular docking, molecular dynamic simulations and ADMET analysis. *J. Mol. Struct.* **1239**, 130488 (2021).
34. Wang, N. *et al.* Network pharmacology-based analysis on bioactive anti-diabetic compounds in Potentilla discolor bunge. *J. Ethnopharmacol.* **241**, 111905 (2019).
35. Liu, Y. *et al.* Integrative analyses of biomarkers and pathways for adipose tissue after bariatric surgery. *Adipocyte* **9**(1), 384–400 (2020).
36. Lai, Y. *et al.* Ganghuo Kanggan decoction in influenza: Integrating network pharmacology and in vivo pharmacological evaluation. *Front. Pharmacol.* **11**, 607027 (2020).
37. Liu, Z.-W. *et al.* Network pharmacology-based investigation on the mechanisms of action of *Morinda officinalis* How. in the treatment of osteoporosis. *Comput. Biol. Med.* **127**, 104074 (2020).

38. Trott, O. & Olson, A. J. AutoDock Vina: Improving the speed and accuracy of docking with a new scoring function, efficient optimization, and multithreading. *J. Comput. Chem.* **31**(2), 455–461 (2010).
39. Kanehisa, M., Sato, Y. & Kawashima, M. KEGG mapping tools for uncovering hidden features in biological data. *Protein Sci.* **31**(1), 47–53 (2022).
40. Chin, C. H. *et al.* cytoHubba: Identifying hub objects and sub-networks from complex interactome. *BMC Syst. Biol.* **8**(Suppl 4), S11 (2014).
41. Oh, K. K., Adnan, M. & Cho, D. H. Network Pharmacology Study on *Morus alba* L. leaves: Pivotal functions of bioactives on RAS signaling pathway and its associated target proteins against Gout. *Int. J. Mol. Sci.* **22**(17), 9372 (2021).
42. Li, S. Network pharmacology evaluation method guidance—Draft. *World J. Tradit. Chin. Med.* **7**(1), 146–154 (2021).
43. Tang, J., Diao, P., Shu, X., Li, L. & Xiong, L. Quercetin and Quercitrin attenuates the inflammatory response and oxidative stress in LPS-induced RAW264.7 cells: In vitro assessment and a theoretical model. *Biomed. Res Int.* **19**, 7039 (2019).
44. Yuan, Z. *et al.* Quercetin rescued TNF-alpha-induced impairments in bone marrow-derived mesenchymal stem cell osteogenesis and improved osteoporosis in rats. *Am. J. Transl. Res.* **10**(12), 4313–4321 (2018).
45. Wei, Y. *et al.* Quercetin prevents oxidative stress-induced injury of periodontal ligament cells and alveolar bone loss in periodontitis. *Drug Des. Dev. Ther.* **15**, 3509–3522 (2021).
46. Park, E. *et al.* Anti-inflammatory activity of herbal medicines: inhibition of nitric oxide production and tumor necrosis factor-alpha secretion in an activated macrophage-like cell line. *Am. J. Chin. Med.* **33**(3), 415–424 (2005).
47. Kim, T. H. *et al.* The effects of luteolin on osteoclast differentiation, function in vitro and ovariectomy-induced bone loss. *J. Nutr. Biochem.* **22**(1), 8–15 (2011).
48. Balci Yuce, H. *et al.* The effect of luteolin in prevention of periodontal disease in Wistar rats. *J. Periodontol.* **90**(12), 1481–1489 (2019).
49. Malaguarnera, L. Influence of resveratrol on the immune response. *Nutrients* **11**(5), 946 (2019).
50. Ribeiro, F. V. *et al.* Resveratrol reverses the negative effect of smoking on peri-implant repair in the tibia of rats. *Clin. Oral Implant Res.* **30**(1), 1–10 (2019).
51. Miossec, P. & Kolls, J. K. Targeting IL-17 and TH17 cells in chronic inflammation. *Nat. Rev. Drug Discov.* **11**(10), 763–776 (2012).
52. Han, Y. K., Jin, Y., Miao, Y. B., Shi, T. & Lin, X. P. CD8(+) Foxp3(+) T cells affect alveolar bone homeostasis via modulating Tregs/Th17 during induced periodontitis: An adoptive transfer experiment. *Inflamm. Res.* **41**(5), 1791–1803 (2018).
53. Lee, H. I. *et al.* Dehydrocostus lactone inhibits NFATc1 via regulation of IKK, JNK, and Nrf2, thereby attenuating osteoclastogenesis. *BMB Rep.* **53**(4), 218–222 (2020).
54. Ding, N. *et al.* Physalin D inhibits RANKL-induced osteoclastogenesis and bone loss via regulating calcium signaling. *BMB Rep.* **53**(3), 154–159 (2020).
55. Hasiakos, S., Gwack, Y., Kang, M. & Nishimura, I. Calcium signaling in T cells and chronic inflammatory disorders of the oral cavity. *J. Dent. Res.* **100**(7), 693–699 (2021).
56. Herath, T. D. *et al.* Porphyromonas gingivalis lipopolysaccharide lipid A heterogeneity differentially modulates the expression of IL-6 and IL-8 in human gingival fibroblasts. *J. Clin. Periodontol.* **38**(8), 694–701 (2011).
57. Boyd, A. R., Shivshankar, P., Jiang, S., Berton, M. T. & Orihuela, C. J. Age-related defects in TLR2 signaling diminish the cytokine response by alveolar macrophages during murine pneumococcal pneumonia. *Exp. Gerontol.* **47**(7), 507–518 (2012).
58. Boyce, B. F. *et al.* TNF-alpha and pathologic bone resorption. *Keio J. Med.* **54**(3), 127–131 (2005).
59. Darabi, E., Kadkhoda, Z. & Amirzargar, A. Comparison of the levels of tumor necrosis factor-α and interleukin-17 in gingival crevicular fluid of patients with peri-implantitis and a control group with healthy implants. *Iran. J. Allergy Asthma Immunol.* **12**(1), 75–80 (2013).
60. Böhm, C. *et al.* RSK2 protects mice against TNF-induced bone loss. *J. Cell Sci.* **125**(Pt 9), 2160–2171 (2012).
61. Ziegler, N. *et al.* Mechano-transduction in periodontal ligament cells identifies activated states of MAP-kinases p42/44 and p38-stress kinase as a mechanism for MMP-13 expression. *BMC Cell Biol.* **11**, 10 (2010).
62. Bradley, L. M., Douglass, M. F., Chatterjee, D., Akira, S. & Baaten, B. J. Matrix metalloprotease 9 mediates neutrophil migration into the airways in response to influenza virus-induced toll-like receptor signaling. *PLoS Pathog.* **8**(4), e1002641 (2012).
63. Carneiro, E. *et al.* Expression analysis of matrix metalloproteinase-9 in epithelialized and nonepithelialized apical periodontitis lesions. *Oral Surg. Oral Med. Oral Pathol. Oral Radiol. Endod.* **107**(1), 127–132 (2009).
64. Campos, K. *et al.* DNA methylation of MMP9 is associated with high levels of MMP-9 messenger RNA in periapical inflammatory lesions. *J. Endod.* **42**(1), 127–130 (2016).
65. Shimada, Y., Ichinose, S., Sadr, A., Burrow, M. F. & Tagami, J. Localization of matrix metalloproteinases (MMPs-2, 8, 9 and 20) in normal and carious dentine. *Aust. Dent. J.* **54**(4), 347–354 (2009).
66. Degidi, M. *et al.* Matrix metalloproteinases 2, 3, 8, 9, and 13 in the peri-implant soft tissues around titanium and zirconium oxide healing caps. *Int. J. Oral Maxillofac. Implants* **28**(6), 1546–1551 (2013).
67. Patel, R. P., Amirisetty, R., Kalakonda, B., Penumatsa, N. V. & Koppolu, P. Influence of smoking on gingival crevicular fluid inter-leukin 1β and interleukin-8 in patients with severe chronic periodontitis among a rural population in India. *Niger. Med. J. J. Niger. Med. Assoc.* **59**(4), 33–38 (2018).
68. Duarte, P. M. *et al.* Could cytokine levels in the peri-implant crevicular fluid be used to distinguish between healthy implants and implants with peri-implantitis? A systematic review. *J. Periodontal Res.* **51**(6), 689–698 (2016).
69. Schierano, G. *et al.* TNF-alpha TGF-beta2 and IL-1beta levels in gingival and peri-implant crevicular fluid before and after de novo plaque accumulation. *J. Clin. Periodontol.* **35**(6), 532–538 (2008).
70. Sakai, A., Ohshima, M., Sugano, N., Otsuka, K. & Ito, K. Profiling the cytokines in gingival crevicular fluid using a cytokine antibody array. *J. Periodontol.* **77**(5), 856–864 (2006).
71. Hirose, K. *et al.* Recombinant interferon-gamma is a potent inhibitor of osteoblastic cell functions. *Meikai Daigaku shigaku zasshi = J. Meikai Univ. Sch. Dent.* **18**(3), 296–301 (1989).
72. Takayanagi, H., Kim, S. & Taniguchi, T. Signaling crosstalk between RANKL and interferons in osteoclast differentiation. *Arthritis Res.* **4**(Suppl 3), S227–S232 (2002).
73. Ralston, S. H., Todd, D., Helfrich, M., Benjamin, N. & Grabowski, P. S. Human osteoblast-like cells produce nitric oxide and express inducible nitric oxide synthase. *Endocrinology* **135**(1), 330–336 (1994).
74. Grewal, T. S., Genever, P. G., Brabbs, A. C., Birch, M. & Skerry, T. M. Best5: A novel interferon-inducible gene expressed during bone formation. *FASEB J.* **14**(3), 523–531 (2000).
75. Duque, G. *et al.* Interferon-γ plays a role in bone formation in vivo and rescues osteoporosis in ovariectomized mice. *J. Bone Miner. Res.* **26**(7), 1472–1483 (2011).
76. Szekanecz, Z., Vegvari, A., Szabo, Z. & Koch, A. E. Chemokines and chemokine receptors in arthritis. *Front. Biosci. (Schol. Ed.)* **2**, 153–167 (2010).
77. Ha, J. *et al.* CXC chemokine ligand 2 induced by receptor activator of NF-kappa B ligand enhances osteoclastogenesis. *J. Immunol. (Baltimore, Md.: 1950)* **184**(9), 4717–4724 (2010).
78. Gamonal, J., Acevedo, A., Bascones, A., Jorge, O. & Silva, A. Characterization of cellular infiltrate, detection of chemokine receptor CCR5 and interleukin-8 and RANTES chemokines in adult periodontitis. *J. Periodontal Res.* **36**(3), 194–203 (2001).
79. Pietruski, J. K., Pietruska, M. D., Stokowska, W. & Pattarelli, G. M. Serum levels of interleukin-1 (IL-1), interleukin-6 (IL-6) and interleukin-8 (IL-8) in patients treated with dental implants. *Rocz. Akad. Med. Bialymst.* **2001**(46), 28–37 (1995).

80. Sánchez-Siles, M., Lucas-Azorin, J., Salazar-Sánchez, N., Carbonell-Meseguer, L. & Camacho-Alonso, F. Salivary concentration of oxidative stress biomarkers in a group of patients with Peri-Implantitis: A transversal study. *Clin. Implant Dent. Relat. Res.* **18**(5), 1015–1022 (2016).

81. Durrani, F. & Singh, R. Myeloperoxidase level around dental implants as an indicator of an inflammatory process. *Indian J. Dent.* **6**(1), 2–6 (2015).

82. Montero, J. *et al.* Peri-implant and paracrestal inflammatory biomarkers at failing versus surviving implant sites in a beagle dog study. *Int. J. Oral Maxillofac. Implants* **32**(4), 807–813 (2017).

83. Liskmann, S., Zilmer, M., Vihalemm, T., Salum, O. & Fischer, K. Correlation of peri-implant health and myeloperoxidase levels: A cross-sectional clinical study. *Clin. Oral Implant Res.* **15**(5), 546–552 (2004).

84. Hickey, M. J. *et al.* L-selectin facilitates emigration and extravascular locomotion of leukocytes during acute inflammatory responses in vivo. *J. Immunol. (Baltimore, Md.: 1950)* **165**(12), 7164–7170 (2000).

85. Seidelin, J. B., Nielsen, O. H. & Strøm, J. Soluble L-selectin levels predict survival in sepsis. *Intensive Care Med.* **28**(11), 1613–1618 (2002).

86. Suzuki, A., Horie, T. & Numabe, Y. Investigation of molecular biomarker candidates for diagnosis and prognosis of chronic peri-odontitis by bioinformatics analysis of pooled microarray gene expression datasets in Gene Expression Omnibus (GEO). *BMC Oral Health* **19**(1), 52 (2019).

87. Dasgupta, B., Chew, T., deRoche, A. & Muller, W. A. Blocking platelet/endothelial cell adhesion molecule 1 (PECAM) inhibits disease progression and prevents joint erosion in established collagen antibody-induced arthritis. *Exp. Mol. Pathol.* **88**(1), 210–215 (2010).

88. Wei, Y. S. *et al.* Platelet-endothelial cell adhesion molecule-1 gene polymorphism and its soluble level are associated with ischemic stroke. *DNA Cell Biol.* **28**(3), 151–158 (2009).

89. Cheng, G. Y. *et al.* CD31 induces inflammatory response by promoting hepatic inflammatory response and cell apoptosis. *Eur. Rev. Med. Pharmacol. Sci.* **22**(21), 7543–7550 (2018).

90. Liu, Y., Zhang, Z., Li, W. & Tian, S. PECAM1 combines with CXCR4 to trigger inflammatory cell infiltration and pulpitis progression through activating the NF-κB signaling pathway. *Front. Cell Dev. Biol.* **8**, 593653 (2020).

91. Wu, Y., Tworkoski, K., Michaud, M. & Madri, J. A. Bone marrow monocyte PECAM-1 deficiency elicits increased osteoclastogenesis resulting in trabecular bone loss. *J. Immunol. (Baltimore, Md.: 1950)* **182**(5), 2672–2679 (2009).

92. Irie-Sasaki, J. *et al.* CD45 is a JAK phosphatase and negatively regulates cytokine receptor signalling. *Nature* **409**(6818), 349–354 (2001).

93. Qian, D. *et al.* JAK2 and PTPRC mRNA expression in peripheral blood mononuclear cells from patients with systemic lupus erythematosus. *Clin. Rheumatol.* **39**(2), 443–448 (2020).

## Acknowledgements

## Author contributions

C.S. finished the target fishing and manuscript. X.J. for provided GEO data and valuable comments; Z.W. provided figures and docking results. In addition, the authors specifically acknowledge the guidance and insightful ideas provided by Professor Z.J.

## Funding

## Competing interests

The authors declare no competing interests.

## Additional information

**Supplementary Information** The online version contains supplementary material available at https://doi.org/10.1038/s41598-022-12366-3.

**Correspondence** and requests for materials should be addressed to J.Z.

**Reprints and permissions information** is available at www.nature.com/reprints.

**Publisher's note** Springer Nature remains neutral with regard to jurisdictional claims in published maps and institutional affiliations.